Gamow-Teller strength in the $^{208}Pb(p,n)^{208}Bi$ reaction at 134.3 MeV

B. S. Flanders,* R. Madey, B. D. Anderson, A. R. Baldwin, and J. W. Watson
Department of Physics, Kent State University, Kent, Ohio 44242

C. C. Foster
Indiana University Cyclotron Facility, Bloomington, Indiana 47405

H. V. Klapdor and K. Grotz
Max-Planck-Institut für Kernphysik, Heidelberg, Federal Republic of Germany
(Received 22 May 1989)

The excitation-energy distribution of transition strength to 1^+ states was measured for the $^{208}Pb(p,n)^{208}Bi$ reaction at 134.3 MeV for excitation energies up to 38 MeV. Structures observed in neutron time-of-flight spectra with forward-peaked ($\Delta L=0$) angular distributions were identified as 1^+ states, except for the transition to the 0^+ isobaric analog state. The 1^+ strength in these structures was extracted by normalizing the yield above a fitted polynomial background to the Fermi transition strength localized in the isobaric analog state. The Gamow-Teller strength observed in the 1^+ peaks is 56% of the $3(N-Z)$ sum rule when the strength of the β^+ transitions is assumed to be zero; 45% of $3(N-Z)$ is observed in the giant resonance and 10% is observed in structures below the giant resonance. Based on a multipole decomposition analysis, an upper limit on the 1^+ strength in the apparent continuum to 38 MeV of excitation energy is estimated to be 37% of $3(N-Z)$. These results are compared with predictions from a shell model that includes a pairing force and a long-range Gamow-Teller force in both the parent and daughter nuclei.

I. INTRODUCTION

The (p,n) reaction at intermediate energies is an important tool in the investigation of the Gamow-Teller (GT) strength function. The neutron spectrum at 0° from a (p,n) reaction on a 0^+ target is dominated by transitions to 1^+ states with $\Delta J=1$, $\Delta L=0$, and $\Delta S=1$; these quantum numbers are the same as those for an allowed GT transition in β decay. The majority of the observed strength is found in a broad resonance peak, the GT giant resonance (GTGR). Many (p,n) reaction studies on 0^+ target nuclides have shown that the yield in the GTGR above an apparent continuum contains only 50–60% of the strength predicted by a general model-independent sum rule[1,2] for an allowed GT β decay; hence, the GT strength is labeled "quenched."[3,4] Theoretical studies have produced a variety of models to explain the quenching, usually by suggesting a movement of strength from the GTGR to higher excitation energies through the influence of the tensor force,[5] the Δ resonance,[6] meson-exchange currents,[7] or ground-state correlations.[8]

Previous studies[9–11] of the $^{208}Pb(p,n)^{208}Bi$ reaction at intermediate energies achieved only modest energy resolution and thus concentrated mainly on the large isobaric analog state (IAS) and GTGR transitions. In this study, we achieved an energy resolution of ~430 keV (FWHM) with large-volume plastic scintillator detectors[12] which allowed observation of structure in the neutron time-of-flight spectra below the GTGR. As such, we extracted the 1^+ strength in the GTGR, in the structures at excitation energies below the GTGR, and in the apparent continuum underneath and above the GTGR up to ~38 MeV of excitation energy.

All structures in the 0° spectrum that exhibited a forward-peaked ($\Delta L=0$) angular distribution were interpreted as 1^+ transitions, except for the transition to the 0^+ isobaric analog state. The GT strength in each of these 1^+ transitions was extracted from the cross section of the peaks above a fitted polynomial background;[3] in addition, the background was examined through a multipole-decomposition analysis to estimate the cross section of the 1^+ strength found there. These differential cross sections were normalized to the Fermi transition strength concentrated in the IAS transition, which exhausts the $(N-Z)$ sum rule for Fermi transitions, in order to extract reduced transition probabilities.

As measured by the reduced transition probability B(GT) [where B(GT)=3 for the beta decay of the free neutron], the GT strength observed in discrete peaks exhausts 56% of the $3(N-Z)$ sum rule when the β^+ strength is assumed to be negligible. The 56% of $3(N-Z)$ observed in discrete states (GTGR plus low-lying structures) is consistent with previous measurements of GT strength in medium- and heavy-mass target nuclei.[3,4] A multipole-decomposition analysis suggests B(GT) =49.5 as an upper limit on the 1^+ strength in the apparent continuum to 38 MeV. The distribution of the observed strength [in B(GT) units] includes (i) 60.8 in the GTGR, (ii) 12.7 in the structures below (smaller excitation energies) the GTGR, (iii) 1.5 in the apparent continuum below the GTGR (0–10 MeV), (iv) 12.3 in the apparent continuum underneath the GTGR (10–20 MeV), and (v) 35.7 in the continuum above the GTGR (20–38 MeV). The B(GT) strength extracted from the continu-

um has large uncertainties associated with the extraction method as will be described in Sec. IV B.

II. EXPERIMENTAL PROCEDURE

The measurements were carried out at the Indiana University Cyclotron Facility with the beam swinger system.[13] The neutrons were detected in meantimed,[14] NE-102 plastic scintillators[12] located in a detector station 85.8±0.2 m from the target along the zero degree line. The detector array consisted of three detectors, each 1.02 m by 0.508 m by 10.2-cm thick, with a frontal area of 1.55 m^2. Anticoincidence detectors in front of and above the array rejected cosmic rays; the anticoincidence detector in front of the array also vetoed charged particles from the target. The details of the data acquisition system are similar to those described previously.[15]

Unpolarized protons with an energy of 134.3 MeV were incident on a 51.4±2.8 mg/cm^2 thick ^{208}Pb (98.7%) target. Neutron energies were measured by the time-of-flight (TOF) technique with an energy resolution (FWHM) of 430 keV for neutrons of 129 MeV. Time-of-flight spectra were measured at average laboratory angles of 0.3°, 4.0°, and 8.4°. Spectra from each detector in the array were recorded at many pulse-height thresholds ranging from 25 to 90 MeV EE (MeV of equivalent-electron energy). A ^{232}Th source (which emits a 2.6 MeV γ ray) and a calibrated fast amplifier were used to calibrate the pulse-height response of the detectors; periodic checks showed that the calibration drifted by as much as 10% during the run. The deviations about this drift were on the order of 5%. Absolute cross sections extracted at several thresholds (~30, 40, 50, and 60 MeV EE) were the same within statistics.

The energy resolution of 430 kev (FWHM) corresponds to an observed time dispersion of 825 ps. We estimate the contributions to the overall time dispersion to be as follows: (i) the intrinsic time dispersion of the neutron detectors (~300 ps), (ii) the beam-energy spread of 0.15% (~405 ps), (iii) the finite thicknesses of the target (~520 ps) and detectors (~440 ps), and (iv) the dispersion in the timing signal obtained from the cyclotron radio frequency (~350 ps). The contributions from the thicknesses of the target and the detectors are rectangular distributions; the other three contributions are assumed to have Gaussian distributions. Because the standard deviation of a rectangular distribution is equal to the width divided by $(12)^{1/2}$, the FWHM of an equivalent Gaussian is 352 ps for the contribution from the target thickness and 298 ps for the contribution from the detector chickness. The quadrature combination of these five contributions yields a resolution of 768 ps FWHM, which assumes that the resultant distribution is Gaussian.

III. DATA REDUCTION

Presented in Fig. 1 is a neutron time-of-flight (TOF) spectrum measured with a 50 MeV EE threshold at 0.3° from the ^{208}Pb$(p,n)^{208}$Bi reaction at 134.3 MeV. The dominant features of this spectrum are the large narrow peak resulting from the excitation of the 0^+ IAS transition superimposed on the large, broad bump which results from the excitation of the 1^+ Gamow-Teller giant resonance (GTGR); in addition, there are six narrow peaks at low excitation (<6 MeV), a broad-structured bump in the region from 7 to 12 MeV and a broad bump above the GTGR. All of these structures lie on top of a background which is comprised of a combination of the cosmic rays that leak through the anticoincidence detectors, the so-called "wraparound" or overlap neutrons from earlier beam bursts, and continuum neutrons from processes such as quasifree neutron knockout. The peak from prompt γ rays (which was observed with only hardware thresholds) was used as a reference to convert this neutron-TOF spectrum to a neutron-energy spectrum. A kinematic transformation from neutron energy

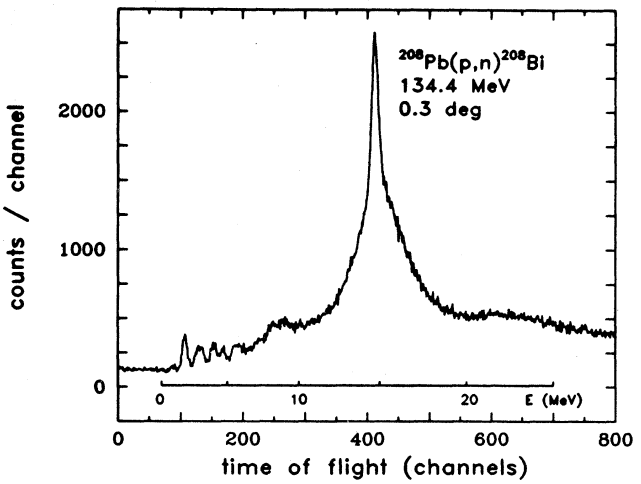

FIG. 1. Neutron time-of-flight spectrum at 0.3° from the ^{208}Pb$(p,n)^{208}$Bi reaction at 134.3 MeV. The inset axis is excitation energy in the final nucleus calibrated from the peak produced by prompt γ rays.

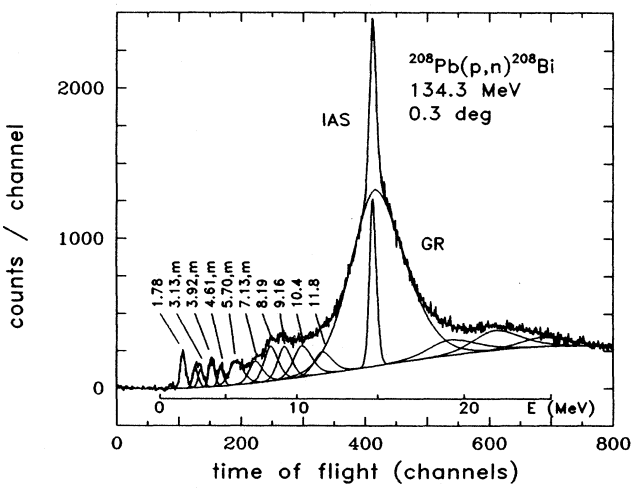

FIG. 2. Neutron time-of-flight spectrum at 0.3° from the ^{208}Pb$(p,n)^{208}$Bi reaction at 134.3 MeV after subtraction of the cosmic ray and wraparound backgrounds. The solid lines are the results from the peak-fitting code ALLFIT as discussed in the text. The peaks containing GT strength are labeled with their excitation energies.

to excitation energy was used to produce the energy scale of Fig. 1.

The computer code ALLFIT (Ref. 16) was used to fit the TOF spectrum with both a polynomial background and several peaks (simultaneously) as shown in Fig. 2. The contributions to the background from cosmic rays and overlap neutrons were subtracted from the spectrum in Fig. 1 to produce the spectrum in Fig. 2. The polynomial background was required to account for the continuum in the region above 30 MeV of excitation energy. A similar background was shown[17,18] for the ^{26}Mg$(p,n)^{26}$Al and ^{40,48}Ca(p,n) reactions to be in good agreement with a normalized plane-wave calculation for quasifree neutron knockout. A similar calculation of the quasifree continuum was not possible for this work because of the lack of knowledge of neutron separation energies for the energy shells of interest here. The line shape chosen for the peaks was an asymmetric hyper-Gaussian of the form

$$\{H \exp[(x-x_0)^{\gamma}/2\sigma_{\pm}^2]\} ,$$

with H, x_0, γ, and $\sigma_{\pm}$ allowed to vary. Here, H is the height, x_0 the position, and σ_+ (σ_-) the width in the positive (negative) x direction. Common shape parameters ($\gamma,\sigma_{\pm}$) were used for all of the peaks; therefore, the line-shape determination was dominated by the large statistical weighting of the IAS and GTGR peaks. The low-lying narrow peaks were fitted with equal (time) widths because their widths should be due primarily to instrumental factors. The broad-structured bump below the GTGR was fitted with five peaks of equal width, and the broad-structured bump in the region above the GTGR was fitted with three peaks of equal width; the choice of five and three was determined subjectively. Because the choice of the number of peaks used to fit the broad bumps is not determined well, the fit to the spectral shape is not unique; however, any equivalent fit with a different number of peaks will produce the same general distribution of strength, which is determined solely from the spectral shape. The excitation energies of the peaks were determined from the fit to the 0.3° spectrum. This determination of excitation energies in the final nucleus is accurate to about 100 keV.

The excitation-energy distribution of the cross section is presented in part (a) of Fig. 3. Absolute cross sections were extracted from the known target thickness, the beam-charge integration, the (Monte Carlo) calculated neutron-detection efficiencies,[19] and the measured solid angle. Corrections to these cross sections were made for the attenuation of the neutron flux in transit and for the computer live time. The beam charge was measured with a well-shielded Faraday cup located approximately 10 m downstream from the target; it is estimated to be accurate to ±5%. The uncertainty in the calculated detection efficiencies is estimated to be about 11%; this is the quadrature sum of 5% uncertainty from the Monte Carlo code and 9% uncertainty in efficiency from the 5% uncertainty in the threshold. The uncertainty in the solid angle is less than 0.5%, which is due largely to the 0.2 m uncertainty in the measured flight path. The attenuation calculation introduces an uncertainty in the cross section of less than ±5%. The estimated systematic uncertainty in the cross sections is ±13%.

IV. GAMOW-TELLER STRENGTH

The total GT strength observed in this reaction was extracted by normalization of the cross section for observed 1^+ GT transitions to the cross section for the Fermi transition to the 0^+ IAS. Because this normalization procedure was described previously,[20] only a review is given here.

For each of the observed sources of GT strength, the ratio of the GT cross section to the Fermi cross section in the IAS transition can be written in the (factorized, zero-range limit) distorted-wave impulse-approximation (DWIA):

$$\frac{\sigma_{\mathrm{GT}}(q_{\min})}{\sigma_F(q_{\min})} = \frac{B(GT)k_f^{\mathrm{GT}}N_D(\mathrm{GT})|V_{\tau}|^2}{B(F)k_f^F N_D(F)|V_{\sigma\tau}|^2} , \quad (1)$$

where B(GT) and B(F) are the reduced transition probabilities for GT and Fermi transitions, k_f^{GT} and k_f^F are the wave numbers of the outgoing neutron for GT and Fermi transitions, N_D(GT) and $N_D(F)$ are the distortion factors from the integration of the distorted waves for GT and Fermi transitions, and $|V_{\tau}|^2$ and $|V_{\sigma\tau}|^2$ are the volume integrals of the effective interactions $V_{\tau}(r)(\tau_1\cdot\tau_2)$ and $V_{\sigma\tau}(r)(\sigma_1\cdot\sigma_2)(\tau_1\cdot\tau_2)$, respectively.

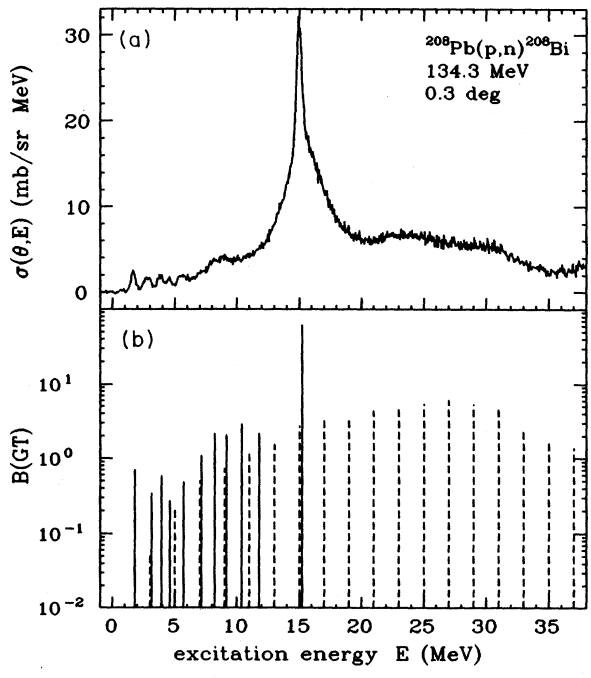

FIG. 3. Excitation-energy distribution of Gamow-Teller strength for the ^{208}Pb$(p,n)^{208}$Bi reaction at 134.3 MeV. Panel (a) is the c.m. cross section distribution for the background-subtracted yield. The solid lines in panel (b) are values of B(GT) extracted from the discrete peaks in the spectrum in panel (a); the dashed lines are the estimated values of B(GT) extracted as described in the text from the apparent continuum described by the polynomial background in Fig. 2.

TABLE I. Center-of-mass cross sections at 0.3° and the associated reduced transition probabilities B(GT) for the $\Delta L=0$ transitions observed with the ^{208}Pb$(p,n)^{208}$Bi reaction at 134.3 MeV.

Excitation energy E_x (MeV)	J^π	Center-of-Mass cross section (mb/sr) $\sigma(0.3°)$	$\sigma_{GT}(0.3°)$	$\sigma_{GT}(q=q_{min})$	Reduced transition probability $B(GT)\pm\Delta B(GT)$[a]
0.84	$L\neq0$	0.12			
1.78	1^+	1.17	1.17	1.19	0.70±0.12
2.72	2^-	0.66			
3.13	mixed	0.59	0.56	0.58	0.34±0.07
3.92	mixed	1.00	0.94	0.99	0.58±0.11
4.61	mixed	0.61	0.43	0.47	0.27±0.06
5.70	mixed	2.06	0.74	0.80	0.48±0.14
7.13	mixed	1.94	1.61	1.80	1.08±0.22
8.19	1^+	3.11	3.11	3.57	2.14±0.39
9.16	1^+	2.90	2.90	3.42	2.06±0.39
10.38	1^+	3.86	3.86	4.72	2.86±0.54
11.77	1^+	2.75	2.75	3.52	2.14±0.44
					Sum (0–12 MeV) 12.65±2.31
15.10 (IAS)	0^+	(8.13)	(8.13)	(11.85)	
15.23 (GR)	1^+	67.41	67.41	98.29	60.84±13.67
					Sum 73.49±15.18
19.92	$L\neq0$	5.38			
22.56	$L\neq0$	7.20			
25.27	$L\neq0$	3.63			

[a]Includes contributions from the peak-fitting process and the extrapolations of σ_{GT} and σ_{IAS} to q_{min}.

In Eq. (1), $\sigma(q_{min})$ is the cross section extrapolated to q_{min}, the kinematic-minimum momentum transfer (0.038 fm^{-1}). This extrapolation was performed with a shape for a $\Delta L=0$ transition to the ground state that is calculated in the DWIA (Ref. 21) with the effective interaction of Franey and Love[22] and the optical potentials of Schwandt *et al.*[23] There is a model dependence to this extrapolation from differences in shapes produced by different wave functions. Several calculations with differing particle-hole contributions were averaged to produce the actual $\Delta L=0$ shape used for the extrapolation. This averaged $\Delta L=0$ shape provided a good description of the momentum-transfer distributions of the transitions labeled 1^+ in Table I. The deviations from the average shape were less than 20% at the momentum transfer of the GTGR and proportionately less for the lower-lying states; hence, the estimated uncertainty in the B(GT) from this extrapolation is less than 20% for the GTGR and less than 10% for the states below 10-MeV excitation energy.

Taddeucci *et al.*[24,25] determined the following relation from comparison of (p,n) reactions with associated β-decay transitions:

$$D(E_p)=\frac{N_D(\mathrm{GT})|V_\tau|^2}{N_D(F)|V_{\sigma\tau}|^2}\simeq\left[\frac{E_p\ (\mathrm{MeV})}{55.0\pm0.4}\right]^2 . \quad (2)$$

For this measurement $D(134.3\ \mathrm{MeV})=5.96\pm0.08$.

The sum rule for allowed 0^+, Fermi ($\Delta L=0,\Delta S=0$) transition strength[1,2] relates the neutron excess of the target to the difference in the strength of β^- and β^+ transitions:

$$S_{\beta^-}(F)-S_{\beta^+}(F)=N-Z\ . \quad (3)$$

The strengths $S_{\beta^\pm}(F)$ are the sums of the reduced transition probabilities $B(F_\pm)$ for $\beta^\pm$ transitions to all possible final states,

$$S_{\beta^\pm}(F)=\sum_f B(F:i^{\beta^\pm}\rightarrow f)=\sum_f\left|\left\langle f\left|\sum_{k=1}^{A}\tau_k^\pm\right|i\right\rangle\right|^2 . \quad (4)$$

Similarly, the sum rule for allowed 1^+, GT ($\Delta L=0,\Delta S=1$) transition strength is

$$S_{\beta^-}(\mathrm{GT})-S_{\beta^+}(\mathrm{GT})=3(N-Z)\ , \quad (5)$$

with

$$S_{\beta^\pm}(\mathrm{GT})=\sum_f B(\mathrm{GT}:i^{\beta^\pm}\rightarrow f)=\sum_f\left|\left\langle f\left|\sum_{k=1}^{A}\boldsymbol{\sigma}_k\cdot\tau_k^\pm\right|i\right\rangle\right|^2 . \quad (6)$$

The reduced transition probabilities are defined such that $B(F)=1$ and $B(\mathrm{GT})=3$ for the beta decay of the free neutron. These sum rules are independent of the structure of the ground state and are based on the assumption that only spin and isospin degrees of freedom are impor-

tant in the nucleus. From the Pauli exclusion principle, one might assume that because the β^+ transitions within the same major shell for this nucleus (with a large neutron excess) are blocked or nearly blocked, the β^+ strength is likely to be small for both Fermi and GT transitions; however, this assumption neglects ground-state correlations which have been shown[8] to be important for ^{208}Pb. MacFarlane[26] predicts that ground-state correlations produce S_{β^+} strength between 25% and 60% of $3(N-Z)$ (these are suggested as lower and upper limits) which requires S_{β^-} strength significantly greater than $3(N-Z)$ to satisfy the sum rule for the ^{208}Pb(p,n) reaction; in the region of the GTGR, he suggests that this increase will be offset approximately by fragmentation of the GT strength which pushes 10–30 % of the strength to higher excitation energies (30–70 MeV).

The Fermi transition strength is concentrated in the IAS so that from Eqs. (3) and (4) with $S_{\beta^+}(F)=0$,

$$S_{\beta^-}(F)=N-Z=B(\mathrm{IAS})\ . \tag{7}$$

This result can be used with Eqs. (1) and (2) to yield

$$B(\mathrm{GT})=\frac{\sigma_{\mathrm{GT}}(q_{\min})}{\sigma_{\mathrm{IAS}}(q_{\min})}\frac{k_f^{\mathrm{IAS}}}{k_f^{\mathrm{GT}}}B(\mathrm{IAS})\frac{N_D(\mathrm{IAS})}{N_D(\mathrm{GT})}\frac{|V_{\sigma\tau}|^2}{|V_\sigma|^2} \tag{8}$$

or

$$B(\mathrm{GT})=\frac{\sigma_{\mathrm{GT}}(q_{\min})}{\sigma\mathrm{IAS}(q_{\min})}\left[\frac{k_f^{\mathrm{IAS}}}{k_f^{\mathrm{GT}}}\right]\frac{(N-Z)}{5.96}\ . \tag{9}$$

The reduced transition probability B(GT) for each GT transition is calculated from Eq. (9) in terms of the extrapolated cross sections. The ratio of $k_f^{\mathrm{IAS}}/k_f^{\mathrm{GT}}$ is in the range from 0.937 for the ground state to 1.001 for the GTGR.

A. GT strength in observed peaks

The center-of-mass cross section extracted at 0.3° from each of the observed peaks is listed in the third column of Table I, whereas the fourth column lists the amount of this cross section associated with a $\Delta L=0$, GT transition. For each of the peaks, average (as just described for the extrapolation) $\Delta L=0$ and $\Delta L=1$ shapes were fitted to the angular distribution of the differential cross section to determine the $\Delta L=0$ strength. The peaks labeled 1^+ in Table I were fit best with no $\Delta L=1$ contribution, while those labeled "mixed" required some $\Delta L=1$ strength to fit the cross-section distribution. The fifth column of Table I contains this extracted GT cross section extrapolated to $q_{\min}$ as described previously. The re-

TABLE II. Center-of-mass cross sections at 0.3° and the associated reduced transition probabilities B(GT) for the $\Delta L=0$ portion of the apparent continuum observed in the ^{208}Pb$(p,n)^{208}$Bi reaction at 134.3 MeV.

Excitation energy E_x (MeV)	Center-of-mass cross section (mb/sr) $\sigma(0.3°)$	$\sigma_{\mathrm{GT}}(0.3°)$	$\sigma_{\mathrm{GT}}(q=q_{\min})$	Reduced transition probability $B(\mathrm{GT})\pm\Delta B(\mathrm{GT})$[a]
2.0–4.0	0.09	0.09	0.09	0.05±0.01
4.0–6.0	0.35	0.35	0.37	0.22±0.04
6.0–8.0	0.75	0.75	0.83	0.50±0.10
8.0–10.0	1.29	1.03	1.21	0.73±0.14
			Sum (2–10 MeV)	1.50±0.23
10.0–12.0	2.02	1.57	1.95	1.19±0.25
12.0–14.0	2.78	1.88	2.50	1.53±0.34
14.0–16.0	3.77	3.09	4.45	2.75±0.67
16.0–18.0	4.88	3.32	5.22	3.26±0.87
18.0–20.0	5.83	3.26	5.64	3.55±1.08
			Sum (10–20 MeV)	12.28±3.35
20.0–22.0	7.16	3.56	6.84	4.35±1.50
22.0–24.0	8.32	3.41	7.34	4.71±1.85
24.0–26.0	9.33	3.42	8.30	5.38±2.42
26.0–28.0	10.40	3.33	9.19	6.02±3.06
28.0–30.0	10.67	2.54	8.02	5.31±3.03
30.0–32.0	10.91	1.89	6.85	4.58±2.91
32.0–34.0	7.59	0.83	3.47	2.34±1.62
34.0–36.0	5.79	0.50	2.42	1.65±1.23
36.0–38.0	6.26	0.36	2.01	1.39±1.09
			Sum (20–38 MeV)	35.73±13.8
			Sum (2–38 MeV)	49.51±15.4

[a]Includes contributions from the multipole decomposition and the extrapolations of σ_{GT} and σ_{IAS} to $q_{\min}$.

duced transition probabilities from Eq. (9) and estimated uncertainties are given in the last two columns of Table I. The excitation-energy distribution of the B(GT) strength observed in the peaks is plotted as the solid lines in panel (b) of Fig. 3. The sum of the β^- strength in the observed peaks, S_{β^-}(GT) is 73.5; the strength in the GTGR is 60.8 and the strength in the low-lying peaks is 12.7. This sum is 56% of $3(N-Z)$, in accordance with previous measurements on medium- and heavy-mass nuclei.[3,4]

B. GT strength in the apparent continuum

The 1^+ strength in the fitted polynomial background was extracted by first binning the yield into 2 MeV wide bins. The time-of-flight spectra cover a range of excitation energy up to 38 MeV. The yield in each bin was converted to a differential cross section, and the angular distribution of the cross section from each bin was fitted to average shapes (as above) calculated in the DWIA at 5, 15, and 25 MeV excitation energy for $\Delta L=0$ and $\Delta L=1$ transitions. Because the momentum-transfer distributions for the low (2–14 MeV) excitation-energy bins are peaked in the forward direction, the extracted B(GT) values are not sensitive to the ambiguities in this ($\Delta L=0,1$) decomposition. We estimate the uncertainties from the decomposition to be on the order of 15% and the uncertainties from the extrapolation to be less than 10%. For the larger (14–38 MeV) excitation-energy bins, the $\Delta L=1$ contributions at 0° are significant and the differences in the shapes for $\Delta L=0$ and $\Delta L=1$ become less distinct so that there is increased sensitivity to the shape ambiguities; we estimate uncertainties on the order of 30% from the decomposition in addition to uncertainties from 15% to 60% from the extrapolation. Moinester[27] provides a detailed discussion of these shape ambiguities in connection with a multipole decomposition analysis of the ^{90}Zr(p,n) reaction at 200 MeV. We observe in Table II that most of the strength in the fitted polynomial background at excitation energies below the GTGR exhibits a $\Delta L=0$ shape, while above the GTGR, a large fraction of the strength is from $\Delta L\neq 0$ transitions. Similarly, measurements of spin-flip probabilities[28] for the ^{40}Ca(p,n) and ^{48}Ca(p,n) reactions suggest that there is only a small amount of 1^+ strength in the continuum from 30 to 45 MeV excitation energy from the excess neutrons in ^{48}Ca. The strength in the continuum is dominated by transitions with multipoles of $\Delta L\geq 1$.

We assign all of the $\Delta L=0$ strength to GT transition strength in accordance with the conclusion of Osterfeld, Cha, and Speth[6] that the forward-angle (p,n) spectra are the result of direct one-step processes only. Because this assignment neglects possible contributions from quasifree scattering, our estimate should be considered an upper limit. The center-of-mass cross section extracted at 0.3° for each of the bins is listed in Table II; also listed are the reduced transition probabilities from Eq. (9) together with the estimated uncertainties. The excitation-energy distribution of the GT strength observed in the continuum is plotted as the dashed lines in panel (b) of Fig. 3. The sum of the β^- strength observed in the apparent continuum at low (0–10 MeV) excitation energies is 1.5, the strength underneath the GTGR (10–20 MeV) is 12.3, and the strength in the background just above the GTGR (18–38 MeV) is 35.7. These values correspond to 1%, 9%, and 27% of $3(N-Z)$, respectively. Thus, an upper limit on the total GT strength observed in the discrete peaks plus the continuum in this reaction is 93±23% of $3(N-Z)$.

A similar analysis[18] of the ^{48}Ca(p,n) reaction at 134 MeV reported observing 43% of $3(N-Z)$ in the discrete peaks and an additional 26% in the residual continuum background (from 4.5 to 30 MeV), which was obtained by subtracting calculated contributions from quasifree scattering. An analysis of spin-flip probabilities for the ^{48}Ca(p,n)^{48}Sc reaction at 0° reveals that the apparent continuum underneath and adjacent to the GTGR is primarily 1^+ strength.[28] The estimated total GT strength from a multipole decomposition of the entire continuum background (to 36 MeV) was 47% of $3(N-Z)$; thus, a total of 90% (with large uncertainties noted for the decomposition) was estimated as an upper limit for the total GT strength in the peaks plus continuum for ^{48}Ca(p,n). An analysis of the ^{76}Ge, ^{82}Se, ^{128,130}Te(p,n) reactions at 134 MeV reported[20] similar strength distributions. The GT strength observed in the peaks as a percentage of $3(N-Z)$ was 55%, 51%, 56%, and 59% with an additional 10%, 7%, 16%, and 12% observed in the continuum background underneath the GTGR for ^{76}As, ^{82}Br, and ^{128,130}I, respectively. Measurements of GT

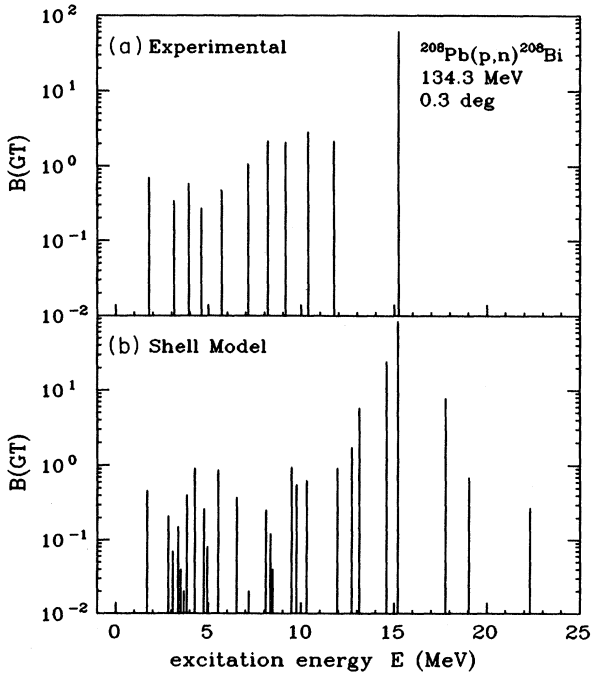

FIG. 4. Comparison of the experimentally observed and predicted excitation energy distribution of GT strength for the ^{208}Pb(p,n)^{208}Bi reaction at 134.3 MeV. The solid lines in panel (a) are the values of B(GT) extracted from the discrete peaks. The solid lines in panel (b) are values of B(GT) from the shell-model predictions of Grotz *et al.* (Ref. 27) discussed in the text.

strength at 135 MeV on lighter targets, with no attempt to estimate the GT strength in the continuum background, showed 67% and 74% of $3(N-Z)$ in the observed peaks for ^{18}F (Ref. 29) and ^{26}Al (Ref. 17), respectively. The larger percentage of $3(N-Z)$ observed in the peaks for these lighter nuclei is due probably to S_{β^+} being significant for these nuclei because ground-state correlations are likely to be important. Madey *et al.*[17] estimate a lower limit of $S_{\beta^+}=0.72$ in the ^{26}Mg$(p,n)^{26}$Al reaction, which means the percentage of the GT sum-rule strength in the peaks is at most 66%. If we assume that $S_{\beta^+}\approx 25\%$ of $3(N-Z)$ for ^{208}Pb (as suggested in Ref. 26), then $\sum B(\mathrm{GT})=123$ is 75% of the GT sum-rule strength.

V. COMPARISON WITH SHELL-MODEL CALCULATIONS

The Gamow-Teller strength function can be calculated with a variety of nuclear models that include extensions to the simple 1p-1h shell model. The calculations presented here are based on the model of Grotz, Klapdor, and Metzinger,[30] which includes ground-state (g.s.) correlations in the target nucleus. This model, described elsewhere,[8,30] includes deviations from simple shell-model ground-state configurations by approximating the distribution of nucleons around the Fermi levels with occupation amplitudes calculated by means of the Bardeen-Cooper-Schrieffer (BCS) theory of superfluid pairing correlations of nucleons.[31] In an earlier work,[8] it was demonstrated that the GT strength distribution in ^{208}Bi is sensitive to small occupations of high-lying neutron orbits and small vacancies in proton orbits. Pairing correlations lead to a coherent contribution of many shells to the transition matrix elements. The 1^+ states in the residual nucleus are calculated in the Tamm-Dancoff approximation which confines the calculation to 1p-1h configurations. The wave functions of the 1^+ states in the residual nucleus are obtained by diagonalizing a Hamiltonian with a long-range residual neutron-proton interaction in the spin-isospin channel. The calculations were performed in a basis large enough to include allowed transitions with unperturbed strength down to about 1% of that for a single-particle transition.

In Fig. 4, we compare the experimental distribution in panel (a) with the strength predicted by Grotz *et al.*[30] in panel (b). In the excitation-energy region below the GTGR (from 0 to 12 MeV), the sum of the observed GT strength in the peaks is 12.7, which is 140% of the sum of the predicted strength. The strength observed in the GTGR is 60.8, which s 50% of the sum of the predicted strength (122.3). Adding the strength in the continuum background underneath the GTGR (from 10 to 20 MeV) increases the strength to 73.1, which is 60% of the predicted strength. The result of this calculation indicates that the quenching of GT strength observed in previous measurements of the (p,n) reaction at intermediate energies is consistent with the expectation of the model of Grotz *et al.*[30] that the quenching is associated with the giant resonance and not with the low-lying strength. This quenching is consistent also with the suggestions[6,31,22] that part of the GT strength from the region of the GTGR is pushed to excitation energies well beyond that predicted by the 1p-1h model.

VI. CONCLUSIONS

Based on a detailed analysis of the GT strength distribution in the ^{208}Pb$(p,n)^{208}$Bi reaction at 134.3 MeV, we estimate that an upper limit on the total GT strength observed below 38 MeV of excitation energy is 93 ± 13 % of $3(N-Z)$. This result includes 10% in transitions below the GTGR, 46% in the GTGR transition, and an estimate of (up to) 37% in the continuum background up to 38 MeV of excitation. These results are additional evidence that the strength observed in 1^+ transitions at excitation energies below the GTGR and the 1^+ strength in the continuum background contribute significantly to the total observed strength. The strength distribution is in general agreement with a shell-model prediction, except that the strength in the region of the GTGR is quenched in the sense that only 60% of the predicted strength is observed. The strength in the low-lying transitions appears not to be quenched, in agreement with a prediction concerning the effect of Δ's in the nucleus.[30] We note also that configuration mixing with multiparticle-multihole states in the continuum[30,33] causes the GTGR to be quenched more than the low-lying states. The 93% total strength observed is in agreement with other measurements on medium-mass nuclei[20] ($A=76$ to 130) when the continuum strength is included. An estimate[26] that $S_{\beta^+}\gtrsim 25\%$ of $3(N-Z)$ then indicates that the total observed GT strength is less than 75% of the GT sum-rule strength.

ACKNOWLEDGMENTS

This research was supported in part by the National Science Foundation under Grant Nos. PHY 85-01054, PHY 88-02392 and PHY 86-11210.

*Present address: Department of Physics, The American University, Washington, D.C. 20016.

[1] K. I. Ikeda, S. Fujii, and J. I. Fujita, Phys. Lett **3**, 271 (1963).

[2] C. Gaarde, J. S. Larsen, M. N. Harakeh, S. Y. van der Werf, M. Igarashi, and A. Müller-Arnke, Nucl. Phys. **A334**, 248 (1980).

[3] R. Madey, B. D. Anderson, B. S. Flanders, and J. W. Watson, in *Weak and Electromagnetic Interactions in Nuclei,* edited by H. V. Klapdor (Springer-Verlag, Berlin, 1986), p. 280; R. Madey, Max-Plank-Institut für Kernphysik Report MPI H-1986-V9, 1986; B. S. Flanders, Ph.D. dissertation, Kent State University, 1985.

[4] J. W. Watson, W. Pairsuwan, B. D. Anderson, A. R. Baldwin, B. S. Flanders, R. Madey, R. J. McCarthy, B. A. Brown, B. H. Wildenthal, and C. C. Foster, Phys. Rev. Lett. **55**, 1369 (1985); C. Gaarde, J. S. Larsen, and J. Rapaport, in *Spin Excitations in Nuclei,* edited by F. Petrovich *et al.* (Plenum, New York, 1984), p. 65; C. D. Goodman and S. D. Bloom, *ibid.*, p.

143.
[5]K. Takayanagi, K. Shimizu, and A. Arima, Nucl. Phys. **A226**, 282 (1974).
[6]F. Osterfeld, D. Cha, and J. Speth, Phys. Rev. C **31**, 372 (1985).
[7]I. S. Towner and F. C. Khanna, Nucl. Phys. **A226**, 282 (1983).
[8]K. Grotz, H. V. Klapdor, J. Metzinger, R. Madey, W. Pairsuwan, B. D. Anderson, A. R. Baldwin, B. S. Flanders, C. Lebo, J. W. Watson, and C. C. Foster, Phys. Lett. **126B**, 417 (1983).
[9]D. J. Horen, C. D. Goodman, C. C. Foster, C. A. Goulding, M. B. Greenfield, J. Rapaport, D. E. Bainum, E. Sugarbaker, T. G. Masterson, F. Petrovich, and W. G. Love, Lett. **95B**, 27 (1980).
[10]C. Gaarde, J. Rapaport, T. N. Taddeucci, C. D. Goodman, C. C. Foster, D. E. Bainum, C. A. Goulding, M. B. Greenfield, D. J. Horen, and E. Sugarbaker, Nucl. Phys. **A369**, 258 (1981).
[11]B. E. Bonner, J. E. Simmons, C. R. Newsom, P. J. Riley, G. Glass, J. C. Hiebert, M. Jain, and L. C. Northcliffe, Phys. Rev. C **18**, 1418 (1978).
[12]R. Madey, J. W. Watson, M. Ahmad, B. D. Anderson, A. R. Baldwin, A. L. Casson, W. Casson, R. A. Cecil, A. Fazely, J. M. Knudson, C. Lebo, W. Pairsuwan, P. J. Pella, J. C. Varga, and T. R. Witten, Nucl. Instrum. Methods **214**, 401 (1983).
[13]C. D. Goodman, C. C. Foster, M. B. Greenfield, C. A. Goulding, D. A. Lind, and J. Rapaport, IEEE Trans. Nucl. Sci. **NS-26**, 2248 (1979).
[14]A. R. Baldwin, and R. Madey, Nucl. Instrum. Methods **171**, 149 (1980).
[15]A. Fazely, M. Ahmad, B. D. Anderson, A. R. Baldwin, A. M. Kalenda, R. J. McCarthy, J. W. Watson, R. Madey, W. Bertozzi, T. N. Buti, J. M. Finn, M. A. Kovash, B. Pugh, and C. C. Foster, Phys. Rev. C **25**, 1760 (1982).
[16]J. J. Kelly, computer code ALLFIT (unpublished).
[17]R. Madey, B. S. Flanders, B. D. Anderson, A. R. Baldwin, C. Lebo, J. W. Watson, S. M. Austin, A. Galonsky, B. H. Wildenthal, and C. C. Foster, Phys. Rev. C **35**, 2011 (1987).
[18]B. D. Anderson, T. Chittrakarn, A. R. Baldwin, C. Lebo, R. Madey, P. C. Tandy, J. W. Watson, B. A. Brown, and C. C. Foster, Phys. Rev. C **31**, 1161 (1985).
[19]R. Cecil, B. D. Anderson, and R. Madey, Nucl. Instrum. Methods **161**, 439 (1979).
[20]R. Madey, B. S. Flanders, B. D. Anderson, A. R. Baldwin, J. W. Watson, S. M. Austin, C. C. Foster, H. V. Klapdor, and K. Grotz, Phys. Rev. C **40**, 540 (1989).
[21]R. Schaeffer and J. Raynal, computer program DWBA70 (unpublished); J. R. Comfort, extended version of DW81 (unpublished).
[22]M. A. Franey and W. G. Love, Phys. Rev. C **31**, 488 (1985).
[23]P. Schwandt, H. O. Meyer, W. W. Jacobs, A. D. Bacher, S. E. Vigdor, M. D. Kaitchuck, and T. R. Donoghue, Phys. Rev. C **26**, 55 (1982).
[24]T. N. Taddeucci, J. Rapaport, D. E. Bainum, C. D. Goodman, C. C. Foster, C. Gaarde, J. Larsen, C. A. Goulding, D. J. Horen, T. Masterson, and E. Sugarbaker, Phys. Rev. C **25**, 1094 (1981).
[25]T. N. Taddeucci, C. A. Goulding, T. A. Carey, R. C. Byrd, C. D. Goodman, C. Gaarde, J. Larsen, D. J. Horen, J. Rapaport, and E. Sugarbaker, Nucl. Phys. **A469**, 125 (1987).
[26]M. H. MacFarlane, Can. J. Phys. **65**, 626 (1987).
[27]M. A. Moinester, Can J. Phys. **65**, 660 (1987).
[28]J. W. Watson, P. J. Pella, A. R. Baldwin, T. Chittrakarn, B. S. Flanders, R. Madey, C. C. Foster, and I. J. van Heerden, Phys. Lett. B **181**, 47 (1986).
[29]B. D. Anderson, A. Fazely, R. J. McCarthy, P. C. Tandy, J. W. Watson, R. Madey, W. Bertozzi, T. N. Buti, J. M. Finn, J. J. Kelly, M. A. Kovash, and B. Pugh, Phys. Rev. C **27**, 1387 (1983).
[30]K. Grotz, H. V. Klapdor, and J. Metzinger, Phys. Lett. **132B**, 22 (1983).
[31]V. G. Soloviev, *Theory of Complex Nuclei* (Pergamon, Oxford, 1976).
[32]A. Klein, W. G. Love, and N. Auerbach, Phys. Rev. C **31**, 710 (1985).
[33]G. F. Bertsch and I. Hamamoto, Phys. Rev. C **26**, 1323 (1982).